A Synchrotron X-ray Diffraction, Neutron Diffraction, ^{29}Si MAS–NMR, and Computational Study of the Siliceous Form of Zeolite Ferrierite

Russell E. Morris,[†,‡] Scott J. Weigel,[†] Neil J. Henson,[†] Lucy M. Bull,[†] Michael T. Janicke,[§] Bradley F. Chmelka,*[,§] and Anthony K. Cheetham*[,†]

Contribution from the Materials Research Laboratory and the Department of Chemical Engineering, University of California, Santa Barbara, California 93106, and The Reactor Radiation Division, National Institute of Standards and Technology, Gaithersburg, Maryland 20899

Received April 25, 1994[⊗]

Abstract: The crystal structure of siliceous zeolite ferrierite has been determined from a combined analysis of synchrotron X-ray and neutron powder diffraction data (space group *Pmnn*, a = 18.7202(1) Å, b = 14.07025(8) Å, c = 7.41971(4) Å, Z = 36, V = 1954.32(2) Å^3, R_{wp} = 12.33%, χ^2 = 3.55). The structure is subtly different from several previously determined aluminosilicate analogues, which were refined in *Immm*, particularly in relation to the absence of a linear Si–O–Si bond angle that is now found to be 170°. The energy minimized structure is in excellent agreement with the experimental results, and the well-resolved ^{29}Si magic-angle spinning NMR spectrum can be assigned on the basis of a bond angle correlation that has been validated for other well-determined siliceous zeolite structures and a 2D INADEQUATE NMR spectrum. This assignment has provided a basis for interpreting the complex NMR spectra that are obtained from aluminosilicate ferrierite samples and enabled us to estimate Si/Al ratios in this multiple T-site system.

Introduction

The zeolite ferrierite (FER) is well-known both in nature and as a synthetic material.[1] Its commercial utility has been restricted by its tendency to contain stacking faults,[2] but interest in its structure and properties has recently been stimulated by a report that it is an excellent shape-selective catalyst for the isomerization of *n*-butenes to isobutene.[3] The latter is an important feedstock for the production of methyl *tert*-butyl ether (MTBE), which is a commercial oxygenate additive in unleaded motor fuel. Ferrierite is typically synthesized as an aluminosilicate with Na,K counter ions, but it has recently been prepared in its siliceous form by a nonaqueous route.[4] The microporous silica polymorphs comprise an important group of materials because they can furnish information that may be vital for understanding the structure and function of a zeolite. For example, their study can yield definitive assignments of ^{29}Si magic-angle spinning (MAS) NMR spectra and thus provide a foundation for interpreting the more complex spectra obtained from aluminosilicate analogues. They also furnish vital reference points for experimental and computational work on sorbate behavior,[5] while in the context of zeolite frameworks, lattice simulation methods for molecular sieves[6,7] are being refined by comparison with the structures of siliceous materials. We describe below a complementary study of the siliceous FER structure by powder neutron diffraction, synchrotron X-ray diffraction, ^{29}Si MAS–NMR, and lattice energy minimization methods. Siliceous zeolite crystal structures that have been elucidated previously include silicalite (MFI),[8] cubic faujasite (FAW),[9] and SSZ-24 (AFI).[10]

The crystal structure of ferrierite was first solved by Vaughan[11] on a magnesium-containing mineral sample from Kamloops Lake, Canada, and has been confirmed by a number of other workers.[2,12] It is closely related to the structures of the mordenite family of zeolites, and is based on five-ring building units, stacked in the [001] direction. These are connected to form oval ten-ring channels running parallel to [001], which are intersected by eight-ring channels running parallel to [010] (Figure 1). Also present in the structure is a small cage, bounded by six-rings, centered at 0,0,0. The space group is reported to be *Immm* (the maximum symmetry of the framework), but this space group imposes restrictions on the structure that have lead to discussion as to whether this is really the true symmetry. Notable among these restrictions is the symmetry-imposed 180° T–O–T (T = Si, Al) bond angle involving the oxygen on an inversion center at $^1/_4,^1/_4,^1/_4$. One study shows abnormal temperature factors for this oxygen, indicating that the apparent 180° bridging bond angle may reflect a statistical distribution of oxygen atoms around, but not coincident with, the center of symmetry. The bridging T–O–T bond angle would then be smaller than 180°, leading perhaps to a more energetically favorable framework conformation.[13,14]

[†] Materials Research Laboratory, UCSB.
[‡] National Institute of Standards and Technology.
[§] Department of Chemical Engineering, UCSB.
[⊗] Abstract published in *Advance ACS Abstracts*, November 15, 1994.

(1) Wise, W. S.; Tschernich, R. W. *Am. Mineral.* **1976**, *61*, 60.
(2) Gramlich-Meier, R.; Meier, W. M.; Smith, B. K. *Zeit. Kristallogr.* **1984**, *169*, 201.
(3) Haggin, J. *C&EN* **1993**, *October 25*, 30.
(4) Kuperman, A.; Nadimi, S.; Oliver, S.; Ozin, G. A.; Garces, J. M.; Olken, M. M. *Nature* **1993**, *365*, 239.
(5) Bull, L. M.; Henson, N. J.; Cheetham, A. K.; Newsam, J. M.; Heyes, S. J. *J. Phys. Chem.* **1993**, *97*, 11776.
(6) Sanders, M. J.; Leslie, M.; Catlow, C. R. A. *J. Chem. Soc., Chem. Commun.* **1984**, 1271.
(7) Henson, N. J.; Cheetham, A. K.; Gale, J. D. *Chem. Mater.* **1994**, *6*, 1647.
(8) Flanigen, E. M.; Bennett, J. M.; Grose, R. W.; Cohen, J. P.; Paton, R. L.; Kirchner, R. M.; Smith, J. V. *Nature*, **1978**, *278*, 512.
(9) Hriljac, J. A.; Eddy, M. M.; Cheetham, A. K.; Donahue, J. A., Ray, G. J. *J. Solid State Chem.* **1993**, *106*, 66.
(10) Bialek, R.; Meier, W. M.; Davis, M. E.; Annen, M. J. *Zeolites* **1991**, *11*, 438
(11) Vaughan, P. A. *Acta crystallogr.* **1966**, *21*, 983.
(12) Alberti, A.; Sabelli, C. *Zeit. Kristallogr.* **1987**, *178*, 249.
(13) Meier, R.; Ha, T. K. *Phys. Chem. Minerals* **1980**, *6*, 37.

0002-7863/94/1516-11849$04.50/0

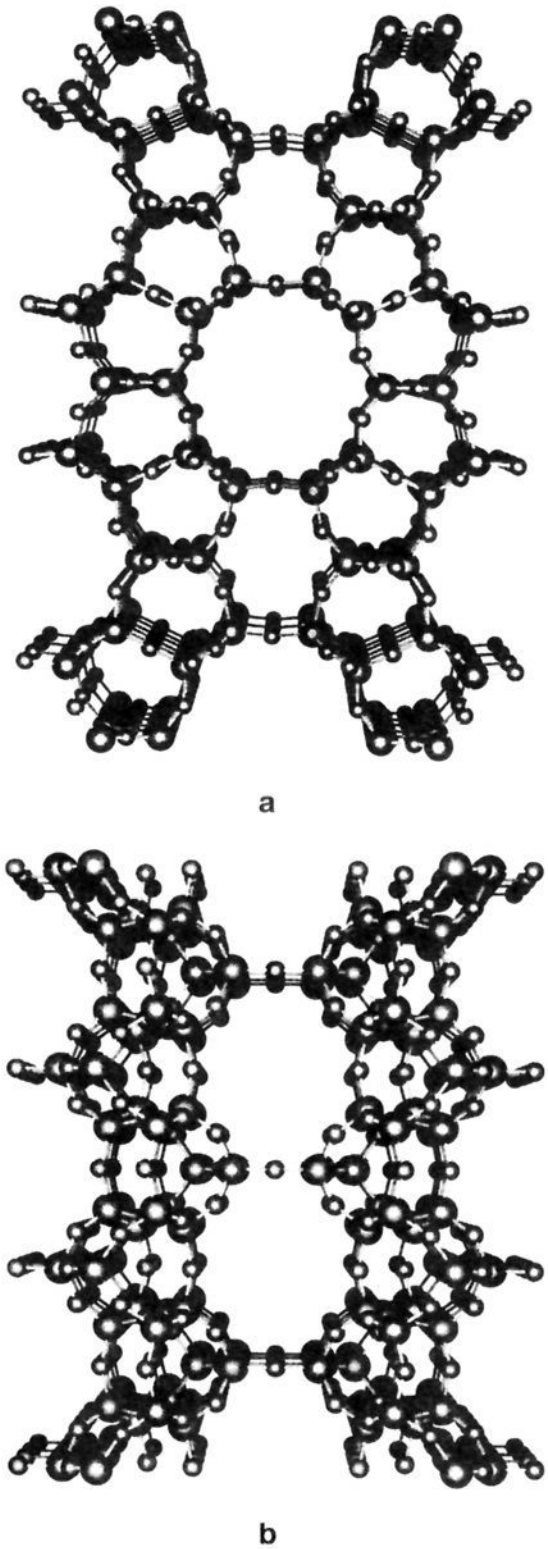

Figure 1. The structure of ferrierite (*Immm* symmetry) viewed (a) down the [001] direction showing the ten-ring channels and (b) parallel to [010] showing the eight-ring channels.

The only structural determination of a ferrierite to show a clear deviation from *Immm* symmetry is that of a monoclinic variety, where a careful single-crystal study by Gramlich–Meier *et al.* indicated a lowering of symmetry to $P2_1/n$ for a naturally occurring Na, K, Mg derivative (the metric symmetry of the unit cell remained orthorhombic).[15] The sample used in the study contained a smaller amount of magnesium than those in the previous experiments, and it was argued that the $Mg(H_2O)_6^{2+}$, which sits in the cage formed by the six-rings, fits so tightly into that cage that it sterically forces the framework into its observed *Immm* symmetry. Diffraction experiments carried out on synthetic ferrierites containing cations of different sizes, and where a lowering of symmetry would be expected, have so far been restricted to powder samples where subtle distortions from the higher symmetry may be more difficult to detect.[16,17] Recently, however, Kuperman and co-workers have produced crystals of a number of all-silica zeolites, including ferrierite, large enough to be analyzed using single-crystal methods.[4] Although they did not report a full structural determination, the space group was reported as showing a reduction of symmetry from *Immm* to *Pmnn* as suggested previously.[13,14]

Experimental Section

1. Synthesis. The hydrothermal crystallization of the siliceous ferrierite was carried out in Teflon-lined 23-mL Parr digestion bombs according to the method of Kuperman et al.[4] The reactants used in the synthesis of ferrierite were pyridine (Fisher), propylamine (Kodak), HF/pyridine (70 wt% HF, Aldrich), Cab-O-Sil (Kodak M-5, scintillation grade), and distilled H_2O. The appropriate amounts of water, propylamine, pyridine, and HF/pyridine were added together first in the Teflon liner, and the clear solution was then stirred for 15 min. After the amines were mixed thoroughly, the silica was added slowly while being continuously stirred. The mixture was then stirred for a further hour to ensure that all the silica was dissolved. The resulting solution was clear and had a pH of 11. The initial mole ratio of oxides was as follows: 1.5 SiO_2:2 HF/pyridine:4 H_2O:8 propylamine:16 pyridine. The autoclave was heated to 170 °C in a forced draft oven with temperature control within 1 °C and left for 7 days to crystallize. After the hydrothermal treatment, the autoclave was removed from the oven and quenched in cold water. The resulting zeolite was separated from its mother liquor by vacuum filtration, washed in deionized water, rinsed with acetone, and dried at room temperature.

The ferrierite isolated from the above synthesis contains organic templates within the channels. To remove the templates, the zeolite was calcined under a 99% oxygen atmosphere in a Lindberg muffle furnace that was ramped at 2 °C/min from room temperature to 850 °C, where it was held for 16 h. The resulting calcined ferrierite was white and showed no evidence of occluded carbon. However, the relatively severe calcination conditions caused the crystals to deteriorate so that only powder diffraction techniques could be applied.

2. Synchrotron X-ray Powder Diffraction. Room temperature synchrotron X-ray powder diffraction data ($6° < 2\theta < 60°$) were collected on beamline X7A at the National Synchrotron Light Source, Brookhaven National Laboratory. The diffractometer operated in triple axis mode, using a Ge(111) monochromator and a Ge(220) analyzer crystal. The mean wavelength was 1.201 86(2) Å. The sample was held in a 1 mm diameter capillary tube and rocked to minimize any preferred orientation and sampling effects. The pattern indicates that the sample contains a very small amount of dodecasil-3C as an impurity.

3. Neutron Powder Diffraction. Room temperature powder neutron diffraction data were collected on diffractometer BT-1 at the National Institute of Standards and Technology, Gaithersburg, Maryland. The mean wavelength used in the experiment was 1.539 Å, selected by using a Cu(311) monochromator.

4. Magic Angle Spinning NMR. Silicon spectra were collected at room temperature on a Bruker AMX 500 spectrometer operating at 11.7 T. A Doty MAS probe was used to spin 5 mm (o.d.) samples at a speed of 6 kHz. A 90° pulse (6 μs) and a 300 s delay were used to acquire 128 transients of 4K data. After a line-broadening of 1 Hz

(14) Gibbs, G. V. *Am. Mineral.* **1982**, *67*, 421.

(15) Gramlich-Meier, R.; Gramlich, V.; Meier, W. M. *Am. Mineral.* **1985**, *70*, 619.

(16) Pickering, I.; Thomas, J. M.; Cheethan, A. K. *J. Catalysis* **1989**, *119*, 261.

(17) Ruschewitz, U.; Cheetham, A. K. Manuscript in preparation.

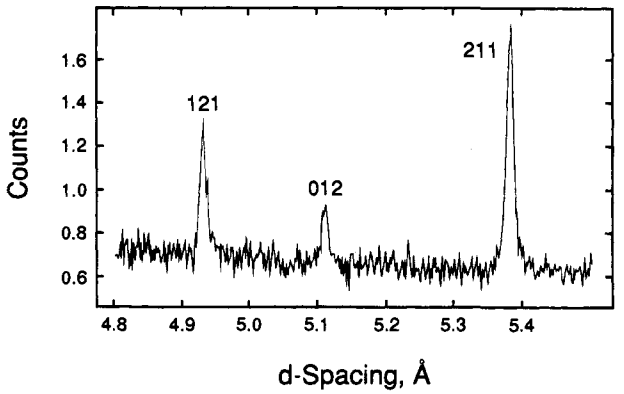

Figure 2. A portion of the synchrotron X-ray diffraction pattern of siliceous ferrierite, showing the presence of the (012) reflection, confirming a lowering of symmetry from body-centered to primitive.

Table 1. Crystallographic Data for Joint Neutron/Synchrotron X-ray Refinement of Siliceous Ferrierite

mol formula	SiO_2	fw	60.084
a	18.7202(1) Å	space group	*Pmnn* (no. 58)
b	14.07025(8) Å	*T*	25 °C
c	7.41971(4) Å	λ(neutrons)	1.539 Å
V	1954.32(2) Å^3	λ(X-rays)	1.201 86 Å
Z	36	R_{wp}[a]	12.33%
R_p[b]	6.90%	χ^2 [c]	3.55
N	14573	*P*	62
C	0		

[a] $R_{wp} = 100\{\sum w_i(y_i - y_{ci})^2/\sum w_i y_i^2\}^{1/2}$. [b] $R_p = 100\sum|y_i - y_{ci}|/\sum|y_i|$. [c] $\chi^2 = \{\sum w_i(y_i - y_{ci})^2/(N - P + C)\}$. Where y_i, y_{ci}, and w_i are the observed intensity, calculated intensity, and weight for the *i*th step. *N* is the number of data points, *P* the number of parameters adjusted, and *C* the number of constraints applied.

was applied, the spectra were zero-filled to 8K, giving a final resolution of 5 Hz per data point. Chemical shifts are referenced relative to TMS. Spectral fitting and simulations were performed using the FELIX software from Biosym Technologies.

The INADEQUATE spectrum was collected with a conventional $[(90°_x)-\tau-(180°)-\tau-(90°)-t_1-(135°)-t_2$, acquire] sequence,[18,19] where the value of τ was chosen to be 16.67 ms ($1/4\ J_{Si-Si}$) and the recycle delay was 10 s. The data were collected in nonphase sensitive mode. Experiments (a total of 64) were carried out with 416 scans in each experiment. The data were processed with sinebell apodization in F1 and Gaussian apodization in F2.

5. Computer Simulations. The program GULP (General Utility Lattice Program), which was developed by Gale,[20] was used to perform symmetry adapted, lattice-energy minimizations of the ferrierite structure in the alternative space groups, *Immm*, *Pmnn*, and $P2_1/n$. All minimizations were performed at constant pressure and used the empirical force-field for silicates developed by Sanders et al.[6] The calculations were performed on Silicon Graphics Challenge XL machine with 128Mb of memory.

Results and Discussion

1. Crystallographic Findings. Initial Rietveld refinement[21] with the synchrotron X-ray data was carried out in space group *Immm*, in accordance with the majority of previously published ferrierite structures. However, close inspection of the Bragg peaks (Figure 2) revealed the presence of weak additional reflections that are forbidden in *Immm*, and the symmetry of the refinement was subsequently lowered to *Pmnn*, in agreement with the findings of Kuperman et al. for the template-containing material.[4] A distance least-squares refinement in *Pmnn* was used to ensure that atoms in the postulated structure were moved off any pseudosymmetric positions, and this model was used as a starting point for subsequent Rietveld calculations. The final least-squares cycle of refinement included terms for a pseudo-Voigt peak shape, lattice parameters, diffractometer zero point, atomic positions, and isotropic temperature factors. There is no justification from the data for a further lowering of symmetry, but we cannot rule out the possibility that additional subtleties remain undetected by powder diffraction methods. The final observed, calculated, and difference plots for the refinement are shown in Figure 3, which also highlights the remarkable amount of detail in the high-angle section of the synchrotron X-ray data.

Table 2. Final Atomic Coordinates and Isotropic Temperature Factors (ESDs in Parentheses) for the Experimental Structure Determination and Final Atomic Coordinates from Calculation

atom	*x*(expt)	*y*(expt)	*z*(expt)	U_{iso}, Å^2
Si(1)	0.15462(34)	0.0	0.0	0.012(4)
Si(2)	0.27439(23)	−0.0012(7)	0.2905(6)	0.013(3)
Si(3)	0.08373(23)	0.19990(33)	0.0037(13)	0.016(2)
Si(4)	0.33150(31)	0.2029(6)	0.2255(8)	0.016(4)
Si(5)	0.68200(33)	0.7950(6)	0.1894(8)	0.006(3)
O(1)	0.2479(6)	0.0	0.5	0.025(6)
O(2)	0.2027(4)	0.0099(11)	0.1788(10)	0.038(5)
O(3)	0.1039(4)	0.0899(5)	0.0016(23)	0.029(4)
O(4)	0.6560(4)	0.7804(5)	−0.0202(18)	0.024(4)
O(5)	0.0	0.2090(9)	0.0377(22)	0.011(6)
O(6)	0.2580(7)	0.2494(10)	0.2851(15)	0.031(5)
O(7)	0.1248(5)	0.2403(8)	0.1829(15)	0.021(5)
O(8)	0.8994(5)	0.7393(8)	0.1675(14)	0.037(6)
O(9)	0.3291(6)	0.0879(10)	0.2462(16)	0.028(7)
O(10)	0.6846(6)	0.9040(10)	0.2477(16)	0.028(6)

atom	*x*(calc)	*y*(calc)	*z*(calc)
Si(1)	0.1512	0.0	0.0
Si(2)	0.2721	−0.0016	0.2923
Si(3)	0.0830	0.2009	0.0130
Si(4)	0.3329	0.1965	0.2226
Si(5)	0.6831	0.7913	0.1896
O(1)	0.2477	0.0	0.5
O(2)	0.2004	0.0131	0.1761
O(3)	0.1007	0.0910	−0.0270
O(4)	0.6548	0.7790	−0.0137
O(5)	0.0	0.2128	0.0616
O(6)	0.2620	0.2465	0.3020
O(7)	0.1285	0.2363	0.1831
O(8)	0.9001	0.7366	0.1649
O(9)	0.3280	0.0829	0.2500
O(10)	0.6863	0.9018	0.2440

Rietveld analysis of the neutron data in space group *Pmnn* showed a statistically significant improvement over that in *Immm*. The refinement included terms for Gaussian peak shape, lattice constants, zero point, atomic positions, and isotropic thermal parameters for both the siliceous ferrierite and for titanium, which is an impurity arising from the sample can. The final observed and calculated patterns are shown in Figure 4.

To obtain the most precise determination of the structure, the X-ray and neutron data sets were combined in a joint Rietveld refinement (the regions where Bragg peaks appear due to the Ti impurity in the neutron data set were excluded from the calculations). Details of the refinement are given in Table 1, final atomic positions and temperature factors in Table 2, and bond distances and angles in Tables 3 and 4, respectively. All Rietveld refinements were carried out using the GSAS suite of programs.[22]

Refinement of the structure in *Pmnn* allows movement of the oxygen (in this case O(6)) from the $^1/_4,^1/_4,^1/_4$ site, so that

(18) Bax, A.; Freeman, R.; Frenkiel, T. A.; Levitt, M. H. *J. Magn. Reson.* **1981**, 43, 478.
(19) Mareci, T. H.; Freeman, R. *J. Magn. Reson.* **1982**, 48, 158.
(20) GULP (the General Utility Lattice Program) written and developed by J. D. Gale, Royal Institution/Imperial College, UK 1992−1994.
(21) Rietveld, H. *Acta Crystallogr.* **1969**, *2*, 65.
(22) Larson, A. C.; Von Dreele, R. B. *Los Alamos Laboratory Report*, **1987**, No. LA-UR-86-748.

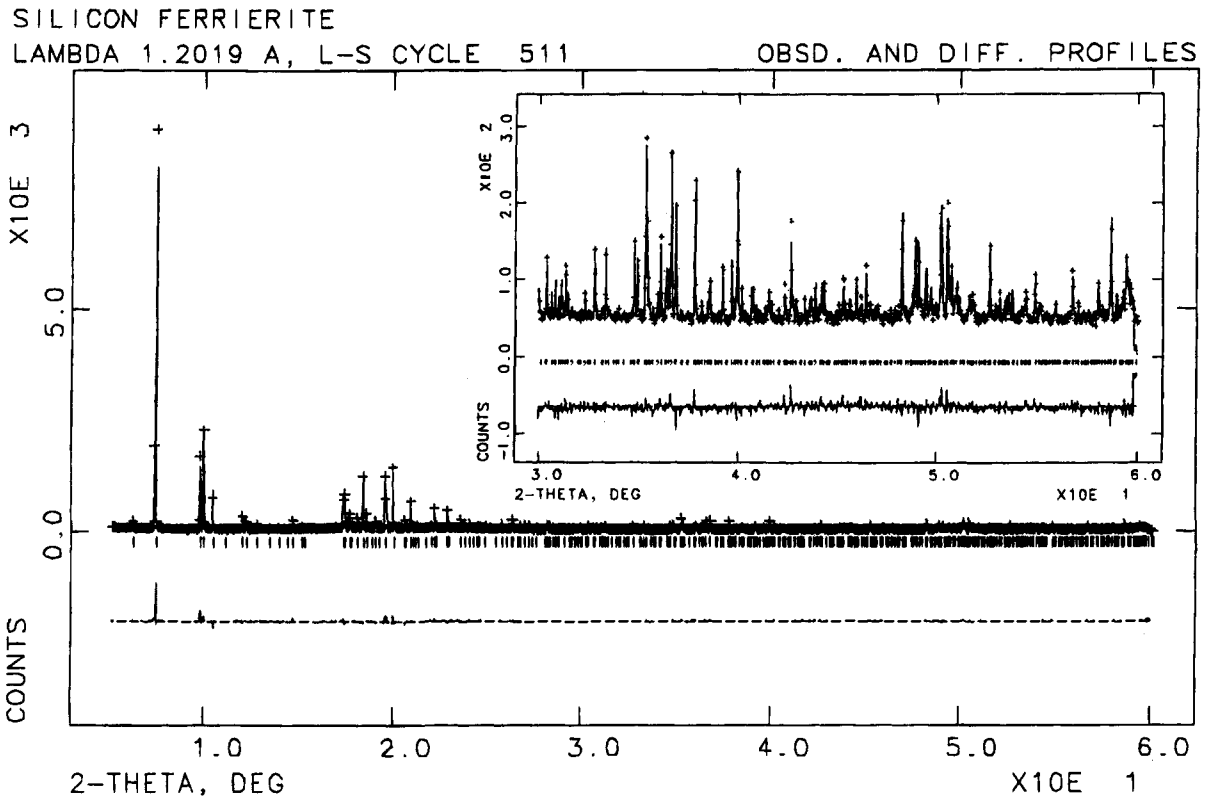

Figure 3. Observed (+), calculated (−), and difference plot for the final refinement of siliceous ferrierite against synchrotron X-ray powder diffraction data. Reflection positions are shown as tick marks. The insert shows the high angle portion of the pattern expanded ×17.

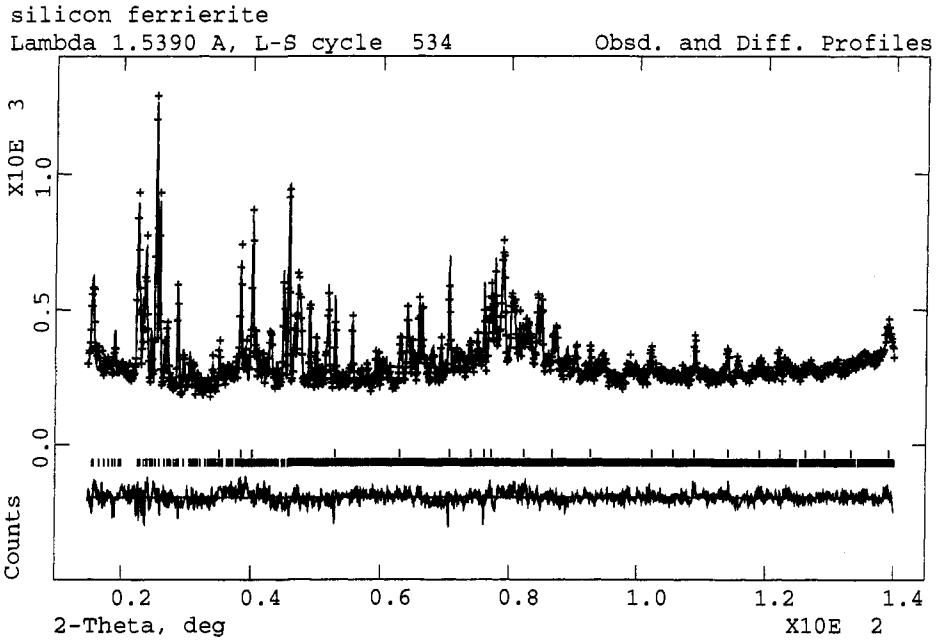

Figure 4. Observed (+), calculated (−), and difference plots for the final refinement of siliceous ferrierite against neutron powder diffraction data. Reflection positions are shown as tick marks for siliceous ferrierite (lower) and titanium metal from the neutron can (upper).

there are no symmetry-imposed 180° Si−O−Si bond angles in the structure. The final refinement shows significant distortions from the *Immm* symmetry (Figure 5), with O(6) moving 0.30 Å away from the $^1/_4,^1/_4,^1/_4$ site, leading to a Si(5)−O(6)−Si(6) bond angle of close to 170°. This is in good agreement with the distortion of this bridge found in monoclinic ferrierite.[15] Other features of the structure are broadly as expected, with average Si−O bond lengths close to 1.60 Å, as is found in other siliceous zeolites.[8-10] The spread of Si−O bond lengths (ca. 1.56−1.65 Å) is somewhat larger than found in other well-characterized siliceous systems (e.g., siliceous FAU:[9] 1.597−1.614 Å), but this is an unavoidable consequence of having a high degree of pseudosymmetry. Paradoxically, refinements in the incorrect *Immm* space group give a much narrower range.

Since there are no extraframework entities present in the title compound, it affords an excellent reference point for comparison with other ferrierite materials. Wise and Tschernich[1] found a strong correlation between the unit cell dimensions and silicon/aluminum content of a number of naturally occurring ferrierite samples. Purely siliceous ferrierite is the end member in this

Table 3. Bond Distances (Å) with ESDs

Si(1)–O(2)	1.609(8)	Si(2)–O(1)	1.632(5)
Si(1)–O(2)	1.609(8)	Si(2)–O(2)	1.585(8)
Si(1)–O(3)	1.581(8)	Si(2)–O(9)	1.652(15)
Si(1)–O(3)	1.581(8)	Si(2)–O(10)	1.572(15)
Si(3)–O(3)	1.594(8)	Si(4)–O(4)	1.559(14)
Si(3)–O(5)	1.593(5)	Si(4)–O(6)	1.586(14)
Si(3)–O(7)	1.637(12)	Si(4)–O(8)	1.584(11)
Si(3)–O(8)	1.563(12)	Si(4)–O(9)	1.625(14)
Si(5)–O(4)	1.643(14)		
Si(5)–O(6)	1.573(13)		
Si(5)–O(7)	1.625(12)		
Si(5)–O(10)	1.593(14)		

Table 4. Bond Angles (deg) with ESDs

O(2)–Si(1)–O(2)	112.0(7)	O(1)–Si(2)–O(2)	103.9(5)
O(2)–Si(1)–O(3)	105.1(7)	O(1)–Si(2)–O(9)	111.7(7)
O(2)–Si(1)–O(3)	114.3(7)	O(1)–Si(2)–O(10)	110.4(7)
O(2)–Si(1)–O(3)	114.3(7)	O(2)–Si(2)–O(9)	110.3(8)
O(2)–Si(1)–O(3)	105.1(7)	O(2)–Si(2)–O(10)	113.0(9)
O(3)–Si(1)–O(3)	106.2(7)	O(9)–Si(2)–O(10)	107.5(5)
O(3)–Si(3)–O(5)	108.2(6)	O(4)–Si(4)–O(6)	109.9(6)
O(3)–Si(3)–O(7)	103.5(8)	O(4)–Si(4)–O(8)	108.7(6)
O(3)–Si(3)–O(8)	118.4(9)	O(4)–Si(4)–O(9)	104.3(7)
O(5)–Si(3)–O(7)	107.8(9)	O(6)–Si(4)–O(8)	115.0(8)
O(5)–Si(3)–O(8)	106.5(8)	O(6)–Si(4)–O(9)	111.1(8)
O(7)–Si(3)–O(8)	112.1(5)	O(8)–Si(4)–O(9)	107.3(7)
O(4)–Si(5)–O(6)	109.3(6)		
O(4)–Si(5)–O(7)	107.3(7)		
O(4)–Si(5)–O(10)	112.8(7)		
O(6)–Si(5)–O(7)	109.5(9)		
O(6)–Si(5)–O(10)	109.4(8)		
O(7)–Si(5)–O(10)	108.5(7)		
Si(2)–O(1)–Si(2)	144.7(8)	Si(1)–O(2)–Si(2)	153.7(8)
Si(1)–O(3)–Si(3)	156.8(6)	Si(4)–O(4)–Si(5)	149.5(6)
Si(3)–O(5)–Si(3)	159.5(14)	Si(4)–O(6)–Si(5)	170.7(9)
Si(3)–O(7)–Si(5)	161.3(9)	Si(3)–O(8)–Si(4)	138.3(8)
Si(2)–O(9)–Si(4)	142.2(8)	Si(2)–O(10)–Si(5)	152.4(9)

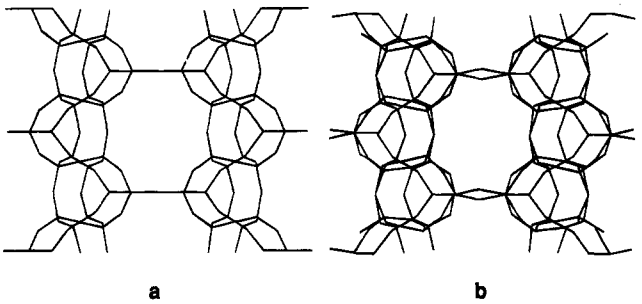

Figure 5. The ferrierite structure viewed parallel to the eight-ring channels ([010] direction) illustrating the distortion of the *Immm* structure (a) on lowering the symmetry to *Pmnn* (b).

system and follows the same relationship as shown in Figure 6. Hydrated magnesium ions have a large effect on the unit cell volume because of their tight fit into the six-ring cages; the influence of other cationic species on the cell volume is somewhat smaller.

2. Computer Simulations. The calculated fractional coordinates of ferrierite in *Pmnn* show excellent agreement with the experimentally determined values (Table 2), as indeed they do for the less complex structure of siliceous faujasite.[7] Furthermore, the calculated cell parameters (a(calc) = 18.576 Å, b(calc) = 13.995 Å, c(calc) = 7.391 Å) are comfortably within 2% of the experimentally observed values (Table 1). Not surprisingly, the Si–O bonds in the energy minimized structure are more regular than in the experimental structure, but the refined bond lengths are all within four esds of the calculated values. The mean bond distances and angles also agree very well: the overall mean Si–O bond distances are 1.599(27) Å

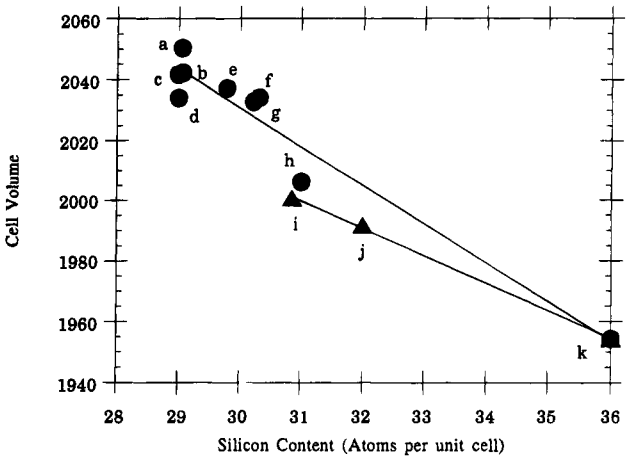

Figure 6. Plot of cell volume (Å^3) vs silicon content of ferrierite for a number of naturally occurring Mg-containing materials (●) and synthetic ferrierites (▲). Samples are from (a) Monte Lake, BC; (b) Francois Lake, BC; (c) Silver Mo., CA; (d) Monastir, Italy; (e) Pinnaeus Lake, BC; (f) Kamloops Lake, BC; (g) Rodolpe Mo., Romania; (h) Sta. Monica Mo., CA (all data from ref 1 except (d) ref 12); (i) synthetic Na,K ferrierite (ref 17); (j) synthetic Na,K ferrierite (ref 17); and (k) siliceous ferrierite.

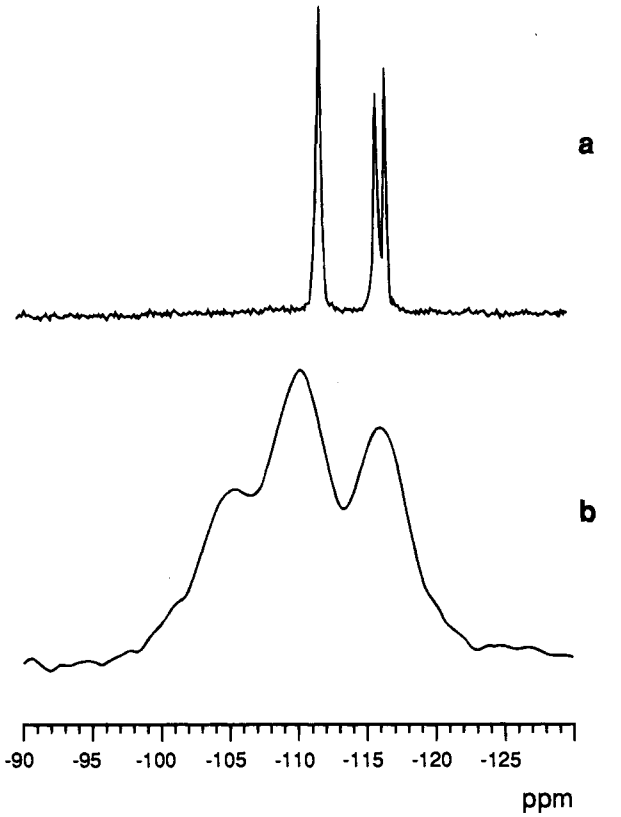

Figure 7. The room temperature ^{29}Si MAS–NMR spectra acquired at 11.7 T of (a) siliceous ferrierite and (b) Na,K ferrierite with Si/Al = 8.

(expt) and 1.599(4) Å (calc); the longest set of Si–O distances are around Si(4) (expt = 1.610(37) Å; calc = 1.602(3) Å) and the shortest are around Si(5) (expt = 1.588(27) Å; calc = 1.595(8) Å). The mean Si–O bond distances around the remaining silicon atoms are Si(1), expt = 1.595(16) Å, calc = 1.598(4) Å; Si(2) expt = 1.597(30) Å, calc = 1.600(4) Å; Si(3) expt = 1.608(31) Å, calc = 1.599(8) Å (figures in parentheses are the standard deviations of the average values). The distortion of the framework from *Immm* is in the same sense in both cases, although movement of O(6) is a little further from $^1/_4,^1/_4,^1/_4$ in

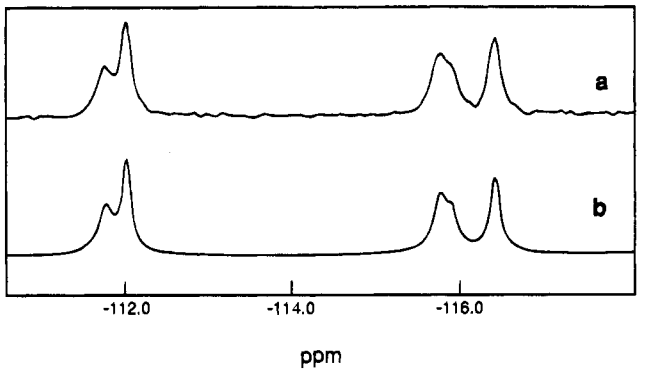

Figure 8. The ^{29}Si MAS–NMR spectra of siliceous ferrierite (a) is compared with the simulated pattern obtained using a five Si site model (b).

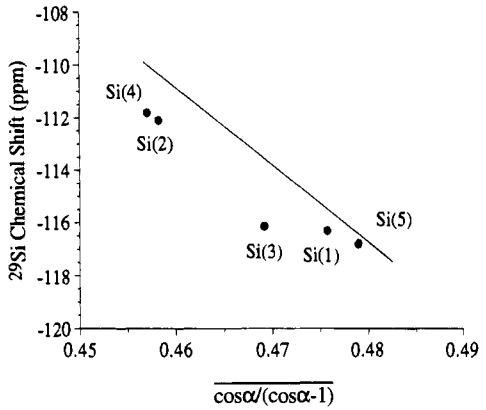

Figure 9. The ^{29}Si chemical shifts for siliceous ferrierite, assigned according to the angular function of the Si–O–Si bond angles, $\cos\alpha/(\cos\alpha - 1)$, are compared with those of zeolite ZSM–5, shown by the full line.[24]

the calculated structure, resulting in a smaller bridging bond angle (160.22°). Calculations performed using space group *Immm* produce a minimized structure that is only marginally higher in energy (~0.5 kJ mol^{-1}) than that in *Pmnn*, reflecting the very subtle differences between the two structural models. The monoclinic $P2_1/n$ structure yields a calculated energy that is almost identical to the *Pmnn* value.

3. ^{29}Si MAS–NMR. The ^{29}Si NMR spectrum of siliceous ferrierite is compared in Figure 7 with the corresponding spectrum of a Na,K ferrierite with Si/Al of ~8. The dramatically enhanced resolution exhibited by the siliceous sample is typical of such comparisons and arises from the absence of disorder due to aluminum substitution into the framework.[23] The space group *Pmnn* requires five different Si sites in the asymmetric unit, one (Si(1)), with a multiplicity of 4, and four (Si(2)–(5)) with a multiplicity of 8; the *Immm* model requires only four. The fives sites are not fully resolved, but the spectrum cannot be fitted to the four site model in *Immm* with required multiplicity ratios of 4:8:8:16. It can be fitted quantitatively to the *Pmnn* model if we allow for the possibility that the five resonances may have different linewidths (Figure 8), but an alternative interpretation based upon the monoclinic $P2_1/n$ structure with nine lines of equal width and intensity gives a comparable fit and cannot be ruled out.

The assignment of the five ^{29}Si resonances to particular T sites in the crystal structure cannot be achieved solely on the basis of the fitting procedure described above because four of the sites have the same multiplicity; only Si(1), with a chemical

(23) Fyfe, C. A.; Strobl, H.; Kokotailo, G. T.; Kennedy, G. J.; Barlow, G. E. *J. Am. Chem. Soc.* **1988**, 110, 3373.

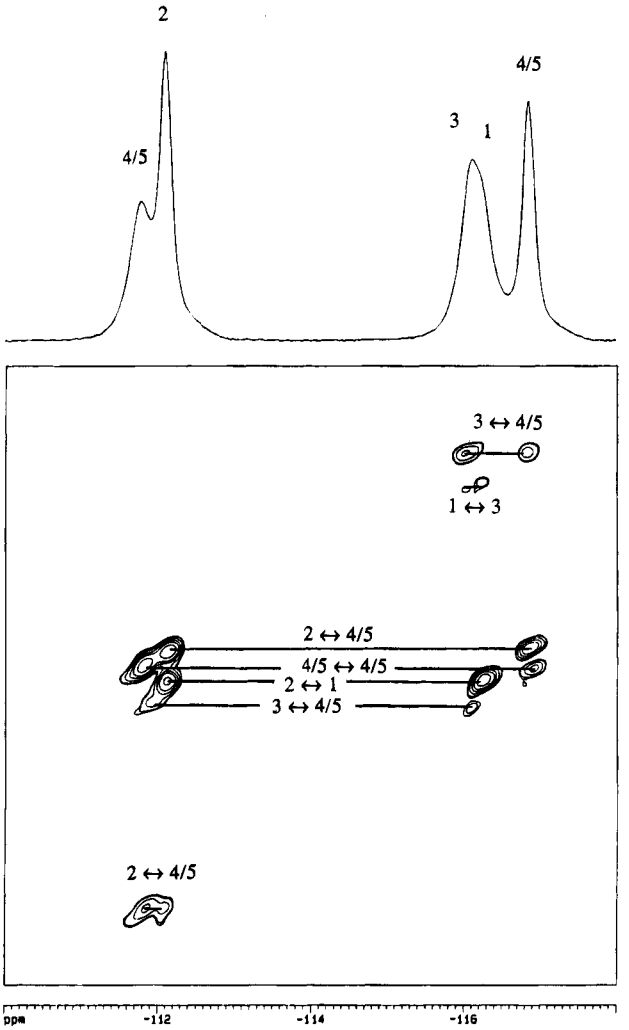

Figure 10. The room temperature ^{29}Si MAS INADEQUATE NMR spectrum acquired at 11.7 T for siliceous ferrierite. The connectivities based on the crystal structure have been used to assign unambiguously silicon sites 1, 2, and 3. Sites 4 and 5 of ferrierite may not be distinguished by this experiment.

Table 5. ^{29}Si MAS–NMR Chemical Shifts and Values for $\cos\alpha/(\cos\alpha - 1)$ (Where α is the O–T–O Bond Angle) at Each Crystallographic T-Site in the Calcined Form of Ferrierite

T-site	^{29}Si MAS–NMR chemical shift	$\cos\alpha/(\cos\alpha - 1)$
Si(1)	−116.3	0.4758
Si(2)	−112.1	0.4583
Si(3)	−116.1	0.4692
Si(4)	−111.8	0.4571
Si(5)	−116.8	0.4790

shift of −116.3 ppm can be assigned from the fitting alone. Recent work by Fyfe[24] and Dupree,[25] however, provides a means of assigning the spectra of siliceous zeolites based upon correlations between the ^{29}Si chemical shifts and certain geometrical features of the structures. In silicalite, for example, correlations between chemical shift and a simple function of the cosine of the average Si–O–Si angle around the particular T site are excellent.[24] Figure 9 shows the results of assigning the spectrum according to this correlation and compares our data with those found in silicalite. The predicted and observed

(24) Fyfe, C. A.; Feng, Y.; Grondey, H. *Microporous Mat.* **1993**, *1*, 393.
(25) Dupree, R.; Cohn, S. C.; Henderson, C. M. B.; Bell, A. M. T. In *Nuclear Magnetic Shielding & Molecular Structure*, NATO ASI; Tossell, J. A., Ed. 1992; Vol. 386, p 421.

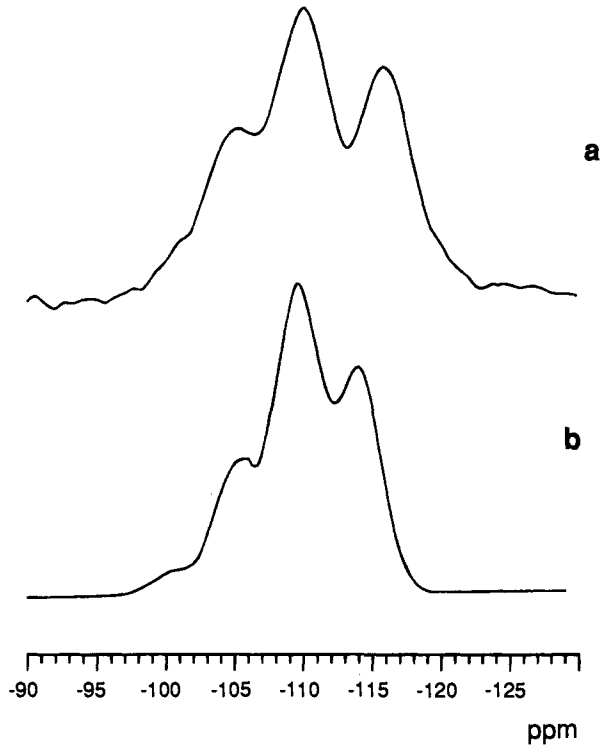

Figure 11. The ^{29}Si MAS–NMR spectra of Na,K ferrierite, Si/Al = 8, (a) is compared with the simulated pattern obtained with a Si/Al ratio of 7 (b).

chemical shifts according to these assignments are presented in Table 5. It is reassuring that the designation of Si(1) on the basis of its multiplicity is consistent with these predictions. These results are also consistent with our 2D INADEQUATE NMR spectrum, shown in Figure 10, which allows us to unambiguously assign the resonances associated with silicon sites 1, 2, and 3. Sites 4 and 5 may not be distinguished using the INADEQUATE experiment as they have the same nearest neighbor Si connectivities. It is interesting to note that the chemical shift/bond angle correlation complements the INADEQUATE spectrum, as Si sites 4 and 5 are readily distinguished by this method.

The above assignments now provide an opportunity to interpret the ^{29}Si NMR spectra from aluminosilicate forms of ferrierite. For example, taking the five T-site model in *Pmnn* and assuming (i) a random distribution of Al, (ii) a downfield shift of 4.5 ppm for each aluminum substituted into the nearest neighbor T-site positions,[26] and (iii) a Gaussian line width of 400 Hz, we can predict the appearance of the corresponding spectrum. Figure 11 shows the results of such a simulation for the Na/K sample with Si/Al~8; the fit shown was obtained using a ratio of 7, confirming that this strategy can be used to estimate Si/Al ratios in multiple T-site systems. The success of this simple approach augurs well for future analyses of aluminum substitution phenomena in complex systems and underlines the value of detailed studies on siliceous zeolitic materials.

Acknowledgment. The work was funded by the MRL program of the National Science Foundation under award DMR 9123048. We thank Martin Attfield for help in collecting the synchrotron X-ray data. N.J.H. thanks the SERC (UK) for a studentship. B.F.C. acknowledges support from the NSF Young Investigator program, the Camille and Henry Dreyfus Foundation, and the David and Lucile Packard Foundation.

(26) Engelhardt, G.; Michel, D. In *High-Resolution Solid-State NMR of Silicates and Zeolites*; Wiley: New York, 1987; p 149.